Opportunity observation of an Algerian Eddy to the south of Cape Palos (southwestern Mediterranean Sea)

Manuel Vargas-Yáñez [1], Ricardo F. Sánchez-Leal [2], Aida Alvera-Azcárate [3], Charles Troupin [3],
Francina Moya [1], Enrique Ballesteros [1], Mariano Serra [4], Rosa Balbín [4], Vicenç Moltó [4],
Mª Carmen García-Martínez [1]

[1] Instituto Español de Oceanografía (IEO-CSIC). Centro Oceanográfico de Málaga. Puerto pesquero de Fuengirola s/n
29640 Fuengirola, Málaga, Spain.
(MV-Y) (Corresponding author) E-mail: manolo.vargas@ieo.csic.es ORCID iD: https://orcid.org/0000-0003-0456-9096
(FM) E-mail: francina.moya@ieo.csic.es. ORCID iD: https://orcid.org/0000-0001-9856-5234
(EB) E-mail: Enrique.ballesteros@ieo.csic.es. ORCID iD: https://orcid.org/ 0009-0009-3148-761X
(MCG-M) E-mail: mcarmen.garcia@ieo.csic.es. ORCID iD: https://orcid.org/0000-0001-6526-9164
[2] Instituto Español de Oceanografía (IEO-CSIC). Centro Oceanográfico de Cádiz, Spain.
(RFS-L) E-mail: rleal@ieo.csic.es. ORCID iD: https://orcid.org/0000-0003-0492-9186
3 Geohydrodynamics and environment research. University of Liege.Bât. B5 Océanographie physiqueAllée du 6 Août 17,
4000, Liège, Belgium.
(AA-A) E-mail: a.alvera@uliege.be. ORCID iD: https://orcid.org/0000-0002-0484-4791
(CT) E-mail: ctroupin@uliege.be. ORCID iD: https://orcid.org/0000-0002-0265-1021
[4] Instituto Español de Oceanografía (IEO-CSIC). Centro Oceanográfico de Baleares. Muelle de poniente s/n, 07015,
Palma de Mallorca, Spain.
(MS) E-mail: mariano.serra@ieo.csic.es. ORCID iD: https://orcid.org/0000-0002-3181-5718
(RB): E-mail: rosa.balbin@ieo.csic.es. ORCID iD: https://orcid.org/0000-0001-5231-1300
(VM) E-mail: vicenc.molto@ieo.csic.es. ORCID iD: https://orcid.org/0000-0002-9918-2216

Summary: Large anticyclonic eddies can detach from the Algerian Current, forming open-sea Algerian Eddies. These mesoscale structures have been intensively studied by means of sea surface temperature and altimetry data, and using numerical models. However, few studies describe an in situ sampling of their whole vertical structure. Furthermore, the area extending from Cape La Nao (western edge of the Balearic Channels) to the Almería-Orán Front has received very little attention, and it could be considered that there is a gap in our present oceanographic knowledge of this part of the western Mediterranean. An Algerian Eddy lasting for several months was detected in December 2021 to the south of Cape Palos. In order to analyse this eddy, an opportunity sampling was designed taking advantage of the periodic monitoring campaign RADMED 0222. This sampling revealed that the eddy had a baroclinic character, affecting the whole water column. These results suggest that this eddy was generated at the Algerian Current, finally affecting an area close to the eastern Spanish coast. The presence of these structures in this region of the western Mediterranean could alter the southward progression of the Northern Current and even the presence and structure of the Almería-Orán Front.

Keywords: Algerian Eddy; Algerian Current; western Mediterranean; mesoscale structures.

Observación de oportunidad de un Giro argelino al sur de Cabo de Palos (Mediterráneo sudoccidental)

Resumen: Giros anticiclónicos de gran tamaño pueden desprenderse de la Corriente Argelina, llegando a formar giros en mar abierto. Estas estructuras de mesoescala han sido estudiadas intensamente mediante datos de temperatura superficial del mar, datos de altimetría, y modelos numéricos. Sin embargo, hay pocos trabajos que describan mediante medidas *in situ* la estructura vertical de estos giros. Al margen de esta circunstancia, la zona que se extiende desde el Cabo La Nao (en el extremo occidental de los Canales Baleares) hasta el Frente Almería-Orán, ha recibido poca atención, pudiéndose considerar que existe una laguna en nuestro conocimiento sobre la oceanografía de esta zona. Un giro anticiclónico fue detectado en diciembre de 2021 al sur de Cabo de Palos, pudiéndose observar durante varios meses. Para analizar este giro se diseñó un muestreo de oportunidad, aprovechando la campaña rutinaria RADMED0222. Este muestreo mostró la estructura baroclina del giro, la cual afectaba a toda su extensión vertical. Los resultados obtenidos también sugieren que el giro se formó en la Corriente Argelina, afectando finalmente a una zona próxima a la costa española. La presencia de este tipo de estructuras en esta región del Mediterráneo Occidental podría afectar a la progresión hacia el sur de la Corriente Septentrional, e incluso a la presencia y estructura del Frente Almería-Orán.

Palabras clave: Giro Argelino; Corriente Argelina; Mediterráneo Occidental; estructuras de mesoescala.

INTRODUCTION

The circulation of the upper layer (0-150 m) of the western Mediterranean (WMED) is dominated by the inflow of fresh Atlantic Water (AW) through the Strait of Gibraltar (Schroeder et al. 2023). In a very simplistic way, it can be stated that part of this current crosses the Alboran Sea (Vargas-Yáñez et al. 2021a), then flows along the Algerian continental slope forming the Algerian Current (AC), and finally enters the eastern Mediterranean (EMED, Fig. 1). Another branch of the AW describes a cyclonic circuit within the WMED, always flowing close to the continental slope of the riparian countries because of the Coriolis force (Millot and Taupier-Letage 2005). However, this simple scheme is severely modified by an intense mesoscale activity. The Atlantic Current frequently describes two anticyclonic gyres in the western (Brett et al. 2020) and eastern sub-basins (Viúdez and Tintoré 1995) of the Alboran Sea, although these structures can disappear, giving rise to different patterns of circulation (Bolado-Penagos et al. 2021, Sánchez-Garrido et al. 2013, Renault et al. 2012). Once in the Algerian Basin, the current detaches from the coast in a northward direction at 4°E, turning to the west and closing a cyclonic circuit centred around 2.5°E/37.5°N. This is known as the Western Algerian Gyre (Cotroneo et al. 2021, Testor et al. 2005). A second cyclonic circuit is centred at 6°E/38.5°N and is named the Eastern Algerian Gyre (Mallil et al. 2022, Cotroneo et al. 2021, Escudier et al. 2016). This current frequently develops cyclonic and anticyclonic eddies, which drift with the main current. While the cyclonic eddies are shallow, affecting only the AW, and have a short life, the anticyclonic ones can reach the sea bottom and last for several months or even years (Puillat et al. 2002). These large anticyclonic eddies can detach from the coast, becoming open-sea eddies (Algerian Eddies, AEs, Escudier et al. 2016), and follow the two cyclonic circuits mentioned above. Although there are still some open questions, such as the mechanisms responsible for the formation of these AEs, their role in the westward transport of intermediate and deep water masses (Mallil et al. 2022, Bosse et al. 2015), and their impact on the biochemistry of this region, our knowledge of the circulation of this area of the WMED has improved considerably during the last few decades.

The branch of the AW that enters the Tyrrhenian Sea completes a cyclonic circuit around the WMED. The northernmost branch of this current is known as the Northern Current and flows along the slope of the Ligurian Sea and in front of the Gulf of Lion before finally turning southwards along the slope of the Catalan Sea. This current is partially deflected northeastwards along the northern coast of the Balearic Islands, forming the North Balearic Current and its associated front, while another part of it continues southwards, mainly along the western side of the Ibiza Channel. The water masses and their circulation through the Balearic Channels have been extensively studied since the 1980s, and several studies have addressed their seasonal (Vargas-Yáñez et al. 2020, Barceló-Llull et al. 2019, Pinot et al. 2002), inter-annual (Pinot et al. 2002), long-term (Vargas-Yáñez et al. 2021b) and high frequency variability (Juza et al. 2019).

The cyclonic circuit followed by the AW (and also by all the other Mediterranean water masses) must finally close when it joins the Almería-Orán Front (AOF). This is an oceanographic structure that has received considerable attention (Troupin et al. 2019, Renault et al. 2012). It separates fresh AW that has recently entered the Mediterranean Sea through the Strait of Gibraltar from the AW that has been severely modified after its circulation around the WMED. It therefore seems logical that the cyclonic circuit closes as shown by the dashed line in Figure 1. However, to our knowledge, there are no specific studies addressing the analysis of water masses and their circulation between Cape La Nao (the western end of the Balearic Channels, see Fig. 1) and the AOF. In May 1998, an anticyclonic eddy centred at 38°N/2°E was detected by means of sea surface temperature (SST) images and altimetry data (Ruiz et al. 2002). This eddy drifted westwards and occupied the area located between Cape La Nao and Cape Palos and was sampled by means of conductivity temperature depth (CTD) and acoustic deep current profiler (ADCP) data and free drifters. To our knowledge, this is the only time that this region has been studied by means of an in situ sampling (at least since the early 1970s). Therefore, it can be concluded that there is a gap in our knowledge of the WMED circulation in this particular area. The circulation scheme proposed in Figure 1 and in other studies (Millot and Taupier-Letage 2005) is not the result of direct observations but of the fact that the AW circuit around the WMED must close. The RADMED project, supported by the Instituto Español de Oceanografía (IEO-CSIC) monitors on a seasonal basis a section of five oceanographic stations (CP1 to CP5, Fig. 2) extending southwards from Cape Palos (Vargas-Yáñez et al. 2017). However, only two of these stations are placed in the open sea. They have been used to estimate the mean properties of water masses and their long-term variability (Vargas-Yáñez et al. 2017), but they are not suitable for filling the gap in our knowledge of the dynamics of the WMED.

In February 2022, an anticyclonic structure characterized by a high SST was detected to the SE of Cape
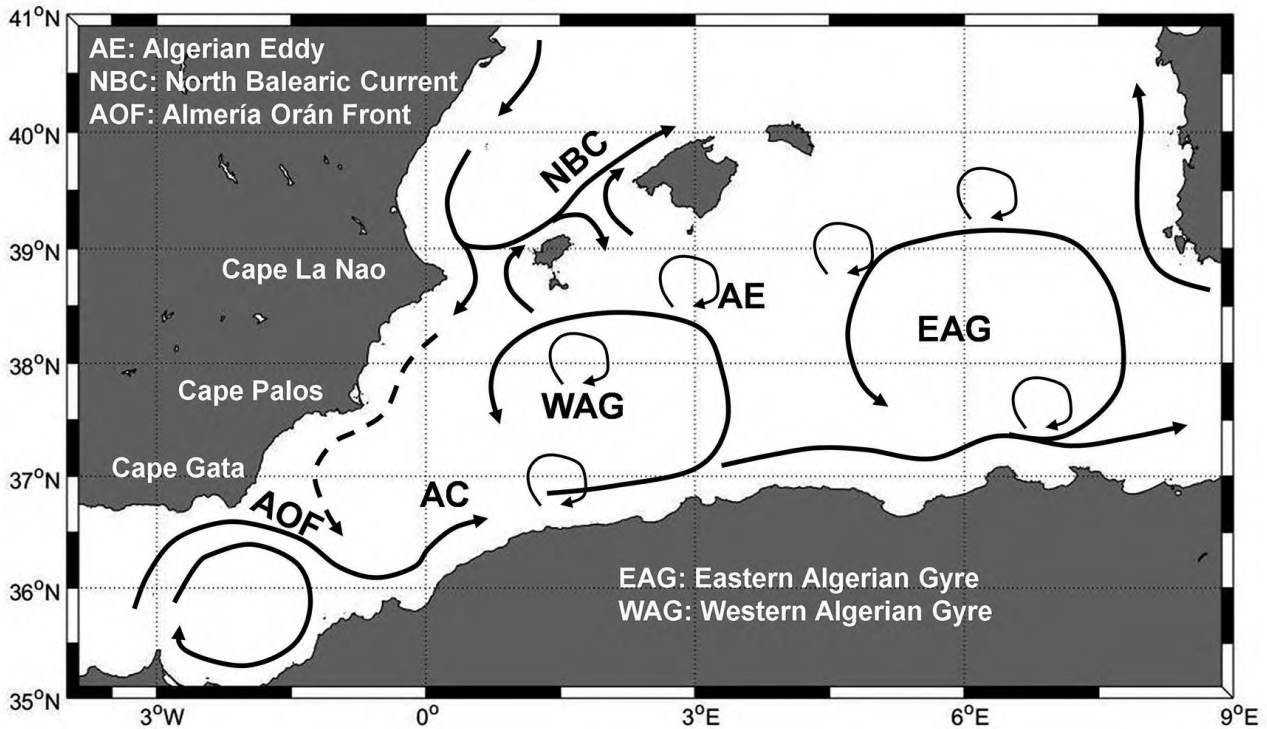
Fig. 1. – Scheme of the circulation in the southwestern Mediterranean Sea.

Palos. The monitoring survey RADMED 0222 offered an opportunity to sample this eddy, contributing to our knowledge of the circulation of water masses between the Balearic Channels and the AOF. Most studies dealing with AEs in this region use remote sensing data and numerical models (Escudier et al. 2016, Isern-Fontanet et al. 2006), but very few of them have sampled the full vertical structure of these eddies. These include the studies of the eddies sampled during the Mediprod-5 survey in May-June 1986 (Millot and Taupier-Letage 2005, Millot et al. 1997) and of the eddy detected to the SE of Cape Palos in May 1998 (Testor et al. 2005, Ruiz et al. 2002). Therefore, the RADMED 0222 survey was used to sample three oceanographic stations within the position of the AE. The present study offers a partial description of the vertical structure of this eddy using CTD, thermosalinograph, ADCP and SST data and the trajectory followed by a turtle equipped with a satellite tracking device.

MATERIALS AND METHODS

The IEO-CSIC carries out a multidisciplinary monitoring programme in the Spanish Mediterranean waters with four oceanographic campaigns per year. The oceanographic stations are distributed along sections which extend from the coast to the open sea (see Vargas-Yáñez et al. 2017 for a detailed description of the positions of these transects). The RADMED 0222 campaign was completed from 23 February to 12 March and included the routine section to the south of Cape Palos (stations CP1 to CP5 in Fig. 2). This section was sampled on 6 March and this opportunity was used to sample three stations within the AE detected on 25

January using SST images. The sampling of stations G1, G2 and G3 was carried out on 7 March. Figure 2B shows the position of this AE on 2 March, when it was centred around 0.25°W and 37.2ªN, with a radius of around 56 km (although it can be tracked further back in time, see results section). Figure 2A shows the positions of the Cape Palos stations and those added for the study of the eddy (G1, G2 and G3).

The campaign was carried out on board the research vessel *Francisco de Paula Navarro* of the IEO-CSIC. This vessel is equipped with a thermosalinograph and a T-RDI 150 KHz Ocean Surveyor hull-mounted ADCP (VM ADCP). The VM ADCP was set for narrow-band single-ping profile mode, using 75 six-metre bins. Data were processed with the University of Hawaii's Common Ocean Data Access System (CODAS; https://currents.soest.hawaii.edu/docs/adcp_doc/). The processing includes referring ADCP velocities to a smooth ocean reference layer, coordinate transformation using an accurate heading source, water-track calibration to obtain an estimate of the heading misalignment and single-ping data editing to screen out bad data (Firing and Hummon 2010). The percent-good data, which indicates the fraction of data that met correlation, error velocity and false target criteria, fell dramatically below the acceptable threshold under 250 m depth. Otherwise, acceptable echo returns were recorded across the top 250 m of the water column. In this study we use full-depth CTD profile data, VM ADCP data, thermosalinograph data and SST satellite images. Thermosalinograph data were regressed on surface CTD data, showing a correlation coefficient of 0.96 for temperature and 0.99 for salinity (see Fig. S1 in supplementary material). Salinity is expressed in the practical salini-
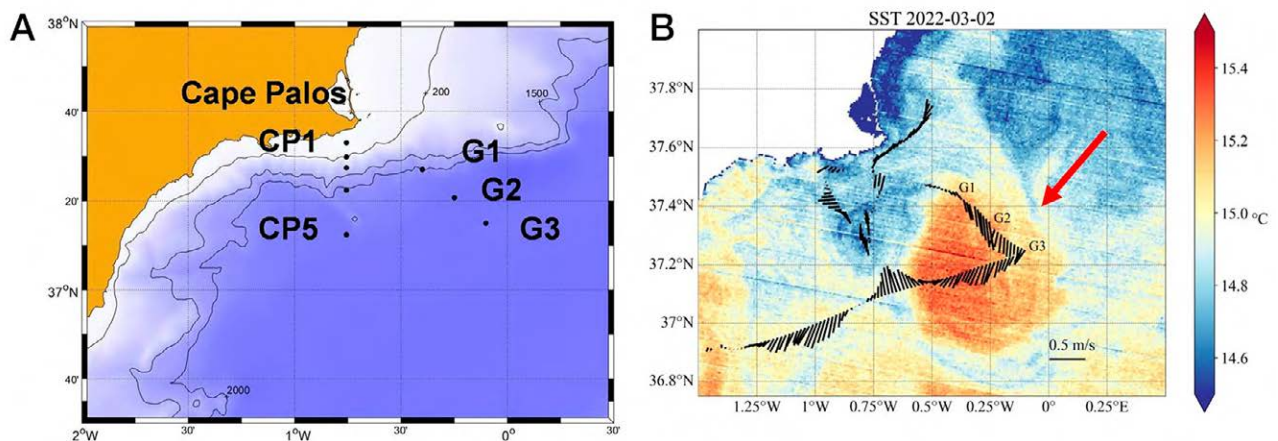
Fig. 2. – A, position of the oceanographic stations for the Cape Palos section and for the three stations devoted to the sampling of the AE. B, the SST corresponding to 2 March 2022, the cloud free image closest to the date of the RADMED sampling. Black sticks are ADCP velocity vectors at the sea surface.

ty scale. Potential temperature is used throughout the study, although the term temperature can be used for brevity. In addition, position data of a turtle equipped with a satellite tracking device were obtained from the website https://seaturtle.socib.es/en/.

Processing of satellite and model data

Satellite SST data were obtained from the multi-sensor Level 3 data provided through the Copernicus Marine Service (CMEMS). In order to obtain a gap-free SST time series to suitably follow the eddy structure, position and strength, these data were reconstructed using data interpolating empirical orthogonal functions (DINEOF), a technique that infers the missing information using a truncated EOF basis obtained through an iterative approach (Beckers and Rixen 2003, Alvera-Azcárate et al. 2005). The optimal number of EOFs is determined using a cross-validation approach: about 3% of the initially valid data are marked as missing, and the number of EOFs that minimizes the root mean square error between the initial data and the DINEOF reconstruction on this dataset is used to make the final reconstruction. The cross-validation data were chosen in the form of clouds (Beckers et al. 2006) to better represent the nature of missing data and obtain a more realistic error estimation. The data covered the period from 1 December 2021 to 31 March 2022, with a daily temporal resolution and a spatial resolution of ~1 km. DINEOF performed a reconstruction retaining 21 EOFs.

In order to examine the probable origin of the eddy, we used a backwards particle tracking approach. Using surface ocean currents from the CMEMS Mediterranean reanalysis product (https://doi.org/10.25423/CMCC/MEDSEA_ANALYSISFORECAST_PHY_006_013_EAS7), we calculated the path taken backwards in time by water particles located at the eddy position using a Runge-Kutta fourth-order method. We used a total of 200 particles over a region of 0.2 degrees centred at

0.25°W, 37.2°N, which is roughly the location of the eddy when it was most developed. The time step used for the particle tracking was 1 hour and the period used was from 29 December 2021 to 28 January 2022.

RESULTS AND DISCUSION

The analysis of the initial and reconstructed SST datasets allows us to study the life cycle of the eddy. The first clear signal of a warm anomaly in the region was on 25 December 2021, and it had a size of approximately 30×45 km and a temperature at its centre of ~16.6°C (Fig. 3A). The signal of the eddy was not clear until 9 January 2022 (Fig. 3B), when it became well defined and had a clear signature (about 0.5°C warmer than the surrounding waters). The eddy then had a more irregular shape (65×46 km) and was at a location to the southwest of the initial position. The eddy was clearly visible during the whole month of February. In some periods it appeared to move offshore (as on 8 February 2022, Fig. 3C). The last time when the eddy was clearly observed by the satellite data was on 9 March 2022 (Fig. 3D), when the it appeared to be already dissipating, because it had lost its circular shape. The region was then completely cloudy from 12 March to 20 March 2022, and the eddy was no longer visible. This long period without data prevented us from establishing with confidence the date on which the eddy finally disappeared, although, according to the DINEOF reconstruction, this may have happened between 14 and 15 March. The average SST for the period 25 December 2021 to 9 March 2022 (Fig. 3E) shows a well-defined eddy located at 0.0542°W, 37.3208°N with a size of 70×55 km, and an average core temperature of 15.4°C.

Figure 4A shows the VM ADCP velocity vectors averaged for the 14 to 32 m layer and for the trajectory followed by the vessel from 5 to 7 March. This figure illustrates the current velocity at the upper layer and corresponds to the average value of the upper four bins of the ADCP data. Figure 4B shows the velocity
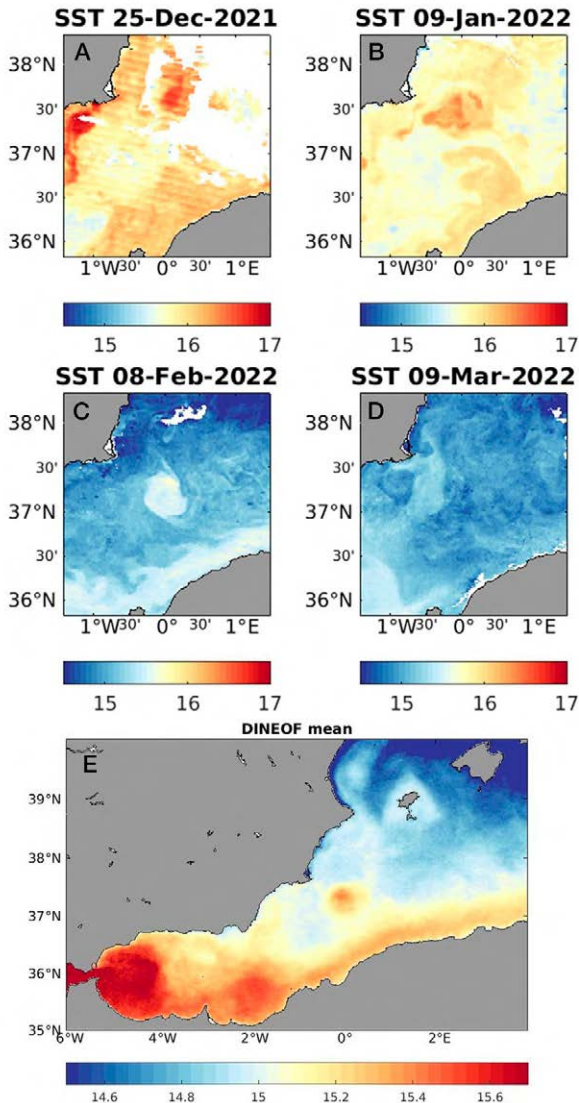
Fig. 3. – SST for 25 December 2021 (A), 9 January 2022 (B), 8 February (C) and 9 March (D). Panel E is the mean SST for the period 25 December to 9 March from the DINEOF reconstruction.
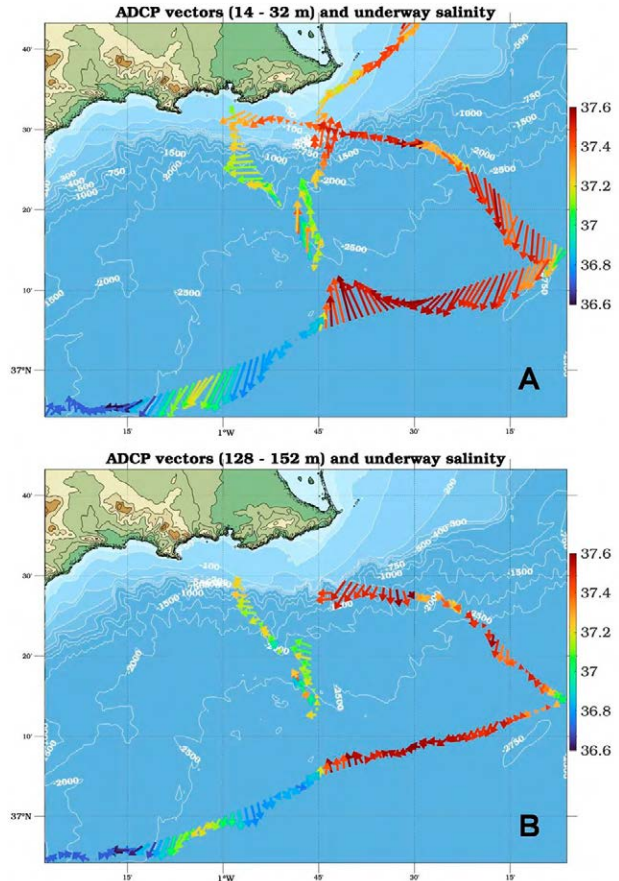

Fig. 4. – A, the arrows are the velocity vectors integrated for the 14-32 m layer. The colour scale shows the surface salinity. B, the arrows are the velocity vectors integrated for the 128-152 m layer. The colour scale shows the surface salinity as in Figure 4A.

vectors averaged for the 128 to 152 m layer, evidencing the decrease in velocity with depth. This layer is close to the detection limit of the instrument, and in this case we considered the average value of five bins to improve the display of the results. Both figures clearly show the clockwise rotation of velocity vectors which characterizes anticyclonic structures. The colour scale in both Fig. 4A and 4B shows the salinity at the sea surface. According to these figures, stations G1 to G3 extended from a central part of the eddy towards its SE end. Therefore, they correspond to the zone of the eddy where the clockwise rotation of the anticyclonic gyre produces the velocity vectors pointing to the southeast to rotate to the southwest. The same results were obtained considering the ADCP velocities up to 250 m, the maximum depth sampled by the ADCP (results not shown).

The salinity values corresponding to this structure were between 37.4 and 37.6 (see colour scale in Fig. 4).

These values, from the thermosalinograph of the vessel, coincide with those obtained from the G1 to G3 CTD stations, which ranged at the sea surface between 37.38 and 37.52. Salinity values measured by the thermosalinograph to the south of Cape Palos ranged between 37.0 and 37.2, also coinciding with results from the CTD profiles. These low salinity values indicate that the water flowing to the south of Cape Palos is fresh AW recently advected into the Alboran Sea through the Strait of Gibraltar that has continued its path directly to the east (Schroeder et al. 2023). The Mediterranean Sea is characterized by a strong net evaporation (Schroeder et al. 2023). This freshwater deficit and the mixing with surrounding waters produce an increase in the AW salinity as it progresses eastwards, reaching values between 37.25 and 37.5 in the Sardinian and Sicilian channels (Schroeder et al. 2023). Unfortunately, there are no clear images corresponding to the initial phase of the eddy (see Fig. 4A), so it could not be tracked to determine its origin, and we can only speculate about it. The lack of continuity in the salinity values observed to the south of Cape Palos and within the eddy suggests that the eddy could have its origin further to the east, and could be an open-sea AE. This salinity increase at the surface of the eddy is also evidenced by the com-
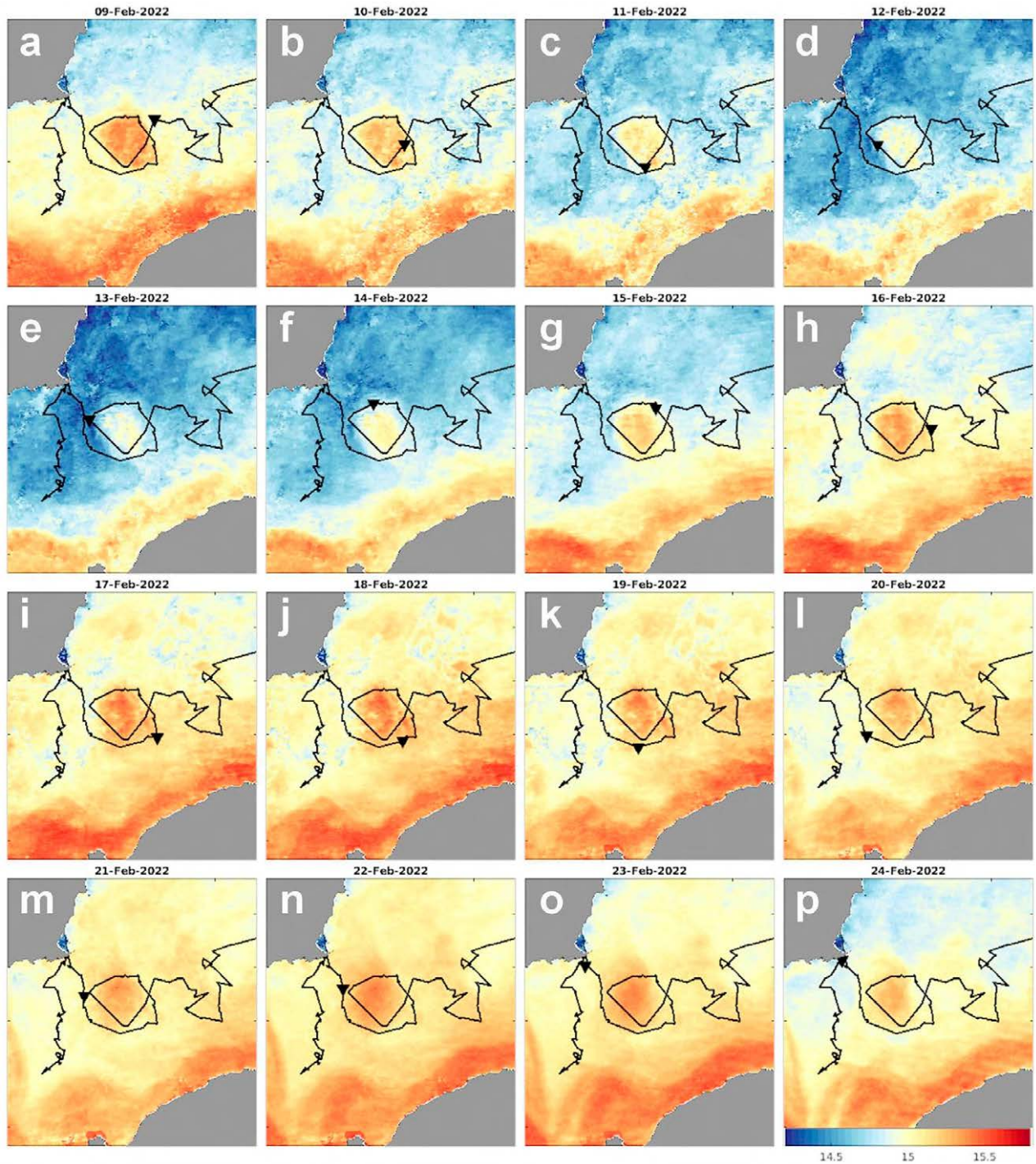
Fig. 5. – The black line is the complete trajectory of the Ashoka turtle. The black triangle is the position of the turtle from 9 February, when it arrived at the eddy, to 24 February, when it left the eddy. The colour scale shows the SST corresponding to each day.

parison of temperature-salinity diagrams from the eddy stations, and those corresponding to the nearby Cape Palos and Cape Gata sections (see Fig. S2 in supplementary material). Brett et al. (2020) and Viúdez et al. (1996) have shown that the maintenance of low salinity values in the inner part of an AW anticyclonic gyre requires the exchange of water with the surrounding current of AW. As the eddy described in this work was detached from the AC, the recirculation of the AW for

several months within this structure would have also increased its salinity. The surface signature of the eddy was evident from satellite and ADCP data. In addition, a loggerhead turtle named Ashoka equipped with a satellite tracking device to monitor its position (https://seaturtle.socib.es/en/) spent about two weeks circling the eddy during the month of February. The path with the underlying SST during these days is shown in Figure 5. Loggerhead turtles can either drift with currents
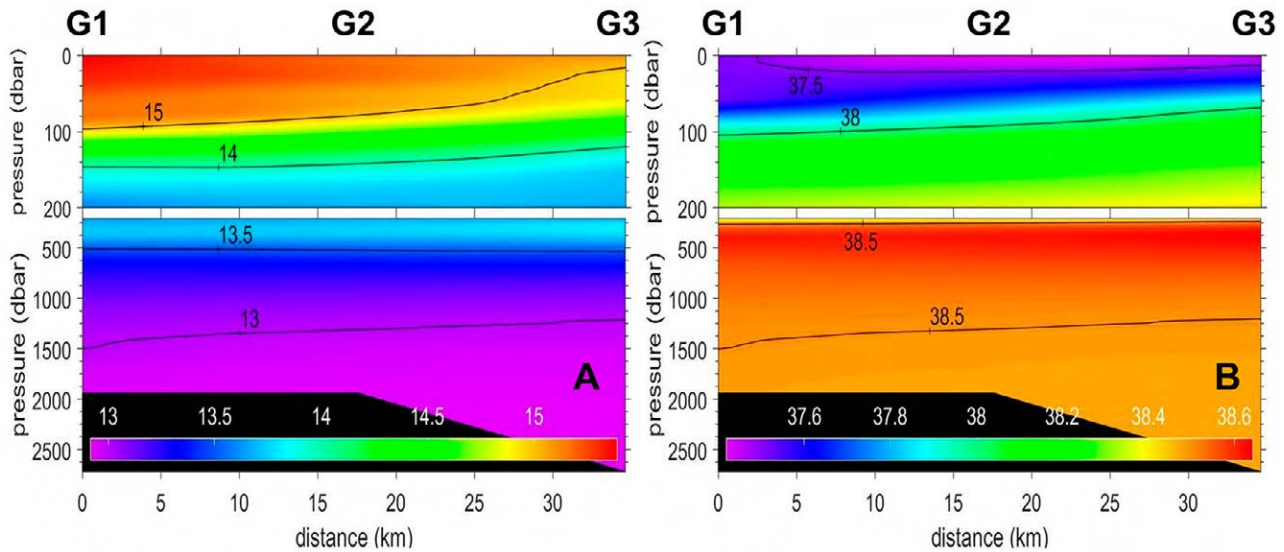
Fig. 6. – A, vertical distribution of potential temperature along the G1-G3 section. B, vertical distribution of salinity for the G1-G3 section.
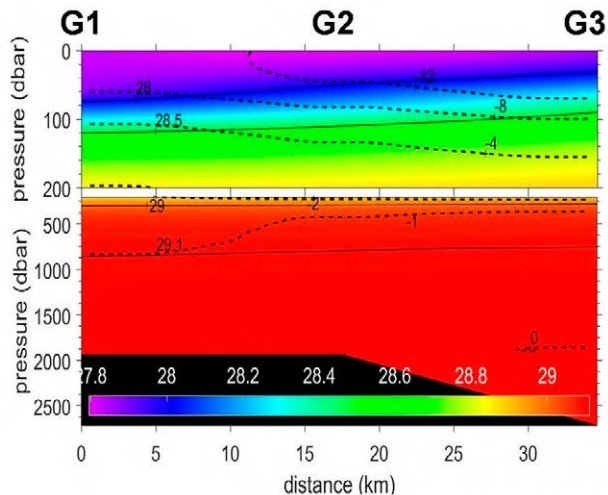

Fig. 7. – Potential density distribution (thick lines and colour scale) for the G1-G3 section, and geostrophic velocity (dashed lines) for the G1-G3 section. Negative velocities are directed off the page, that is, in a SW direction.
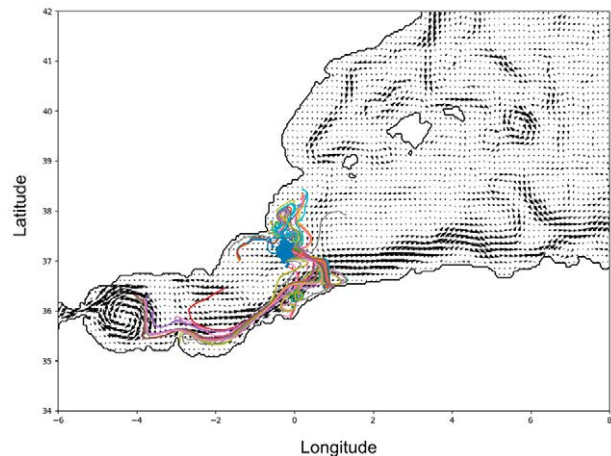

Fig. 8. – Initial position of the 200 particles (blue dots) and back trajectories (coloured lines) indicating the path taken by the water mass located in the vicinity of the eddy in January 2022. The arrows show the average surface currents for the period 29 December 2021 to 28 January 2022.

or swim actively (Scott et al. 2014). During Ashoka's turn around the eddy, it alternated travel periods with others in which it did not move from a given region for a few hours. On 18 February, the turtle advanced during one of the travel periods at a speed of about 0.28 m s⁻¹. Geostrophic water velocity as provided through CMEMS (product SEALEVEL_EUR_PHY_L4_NRT_OBSERVATIONS_008_060) shows speeds of 0.12 to 0.22 m s⁻¹, which could indicate that Ashoka was indeed drifting with the eddy, or swimming slightly, helped by the currents, and we speculate that stopping periods would be for feeding. This example shows that the eddy had a well-defined signature, with currents strong enough to attract the turtle and make it perform a complete circuit around the eddy.

The CTD stations along the eddy section allowed us to observe the vertical structure of this part of the eddy. Figure 6 shows the upward tilting of isotherms and iso-

halines from the central area of the eddy towards its SE extreme. It is clear that this tilting affects all the water masses from the sea surface to the bottom, although it is more pronounced in the upper AW layer. The same structure can be observed in the potential density distribution (thick lines in Fig. 7). The geostrophic velocity on the direction normal to the section shows values that are negative (dashed thin lines), that is, off the page (towards the SW), in agreement with the ADCP data. The geostrophic velocity was calculated using the bottom as the reference layer. These calculations were repeated with a 200 dbar reference, which is usually taken as the no motion level in the nearby Alboran Sea. The results were very similar in both cases.

Based on the results presented above, we speculated that an AE, very likely generated around 1°E, may have drifted westwards and lasted for several months to the SE of Cape Palos. This would be in agreement

with Testor et al. (2005), who considered that AEs are frequently generated between 1°E and 2°E. In order to support this hypothesis, we used a backwards particle tracking approach, using surface ocean currents from the CMEMS Mediterranean reanalysis (see data section for details of the reanalysis product) from 29 December 2021 to 28 January 2022. During that period, water particles located in the Alboran Sea and along the Algerian coast were driven by currents to the eddy region following a sharp offshore turn at a longitude of 1°E, as shown in Figure 8. This trajectory suggests that a filament detached from the Algerian coast, bringing waters from the Algerian Current towards the Spanish coast could be at the origin of the eddy analysed in this study. Part of the particles originated from the vicinity of the eddy, indicating that there was also a recirculation of local waters in the region, facilitating the formation of the eddy.

The vertical structure of two other AEs had previously been sampled by means of CTD data. One of them was located around 5°E in June 1986, and its signature was evident up to 800 m depth (Benzohra and Millot 1995). The other one was sampled in May 1998, to the SE of Cape Palos, and reached the sea bottom (Ruiz et al. 2002). Our results confirm that these AEs can reach the sea bottom. The calculation of geostrophic currents shows a clear decrease with depth from the sea surface. This would also indicate the baroclinic character of these structures, as mentioned by Escudier et al. (2016).

More importantly, the opportunity of sampling an open-sea AE has revealed that the closure of the cyclonic circuit followed by the AW within the WMED may be more complex than the scheme outlined with the dashed line in Figure 1. The average behaviour of the AW may include a southward extension of the Northern Current, closing the cyclonic circuit around the WMED at the AOF (Fig. 1; Millot and Taupier-Letage 2005). This seems to be confirmed by the mean SST distribution in Figure 3E, where the AOF is clearly visible. However, it is very likely that there are exceptions to this circulation scheme, in which the AW does not form a smooth current flowing to the SW along the Spanish continental slope. On the contrary, the transition of the AW, and also of the other Mediterranean water masses, from the Balearic Channels to the AOF, may be affected by an intense mesoscale activity such as the one described in this study from late December 2021 to mid-March 2022. This hypothesis would have important consequences for the circulation of the WMED. First, the presence of AEs close to Cape Palos could temporally block the circulation, and the closure of the cyclonic circuit of the WMED would occasionally not be placed at the AOF, but further north. Notice that the position of the AE described in Ruiz et al. (2002) could represent a blocking situation even clearer than the one presented in this work. Second, the AOF would still be a sharp front separating fresh and "old" AW when this region is not affected by AEs. However, the separation between recent AW and modified AW would be much more diffuse when AEs reach the Spanish coast to

the south of Cape Palos. In such cases, it is very likely that a proper front could not be identified. These different scenarios could also have important implications for the biology of this region, as exemplified by the trajectory of the turtle Ashoka. In any case, it seems clear that the region from the Balearic Islands to Cape Gata is a large geographical area within the WMED that needs further study to fill the present gap in the knowledge of its dynamics and the role of AEs in its circulation.

FINANCIAL SUPPORT

REFERENCES

Alvera-Azcárate A., Barth A., Rixen M., Beckers J.M. 2005. Reconstruction of incomplete oceanographic data sets using empirical orthogonal functions: application to the Adriatic Sea surface temperature. Ocean Modelling 9: 325-346.
https://doi.org/10.1016/j.ocemod.2004.08.001
Barceló-Llull B., Pascual A., Ruiz S., et al. 2019. Temporal and spatial hydrodynamic variability in the Mallorca Channel (Western Mediterranean Sea) from eight years of underwater glider data. J. Geophys. Res. Oceans 124: 2769-2786.
https://doi.org/10.1029/2018JC014636
Beckers J.M., Rixen M. 2003. EOF Calculations and Data Filling from Incomplete Oceanographic Datasets. J. At. Ocean. Techn. 20: 1839-1856.
https://doi.org/10.1175/1520-0426(2003)020<1839:ECADFF>2.0.CO;2
Beckers J.M., Barth A., Alvera-Azcárate A. 2006. DINEOF reconstruction of clouded images including error maps - application to the Sea-Surface Temperature around Corsican Island. Ocean Science 2: 183-199.
https://doi.org/10.5194/os-2-183-2006
Benzohra M., Millot C. 1995. Hydrodynamics of an open sea Algerian eddy. Deep-Sea Res. I. 42: 1831-1847.
https://doi.org/10.1016/0967-0637(95)00046-9
Bolado-Penagos M., Sala I., Gomiz-Pascual J.J., et al. 2021. Revising the effects of local and remote atmospheric forcing on the Atlantic Jet and Western Alboran Gyre dynamics. J. Geophys. Res. Oceans 126: e2020JC016173.
https://doi.org/10.1029/2020JC016173
Bosse A., Testor P., Mortier L., et al. 2015. Spreading of Levantine Intermediate Waters by submesoscale coherent vortices in the northwestern Mediterranean Sea as observed with gliders, J. Geophys. Res. Oceans 120: 1599-1622.
https://doi.org/10.1002/2014JC010263
Brett G.J., Pratt L.J., Rypina I.I., Sánchez-Garrido J.C. 2020. The Western Alboran Gyre: An analysis of its properties and its exchange with surrounding water. J. Phys. Oceanogr. 50: 3379-3402.
https://doi.org/10.1175/JPO-D-20-0028.1
Cotroneo Y., Celentano P., Aulicino G., et al. 2021. Connectivity analysis applied to mesoscale eddies in the Western Mediterranean Basin. Remote Sens. 13: 4228.
https://doi.org/10.3390/rs13214228
Escudier R., Mourre B., Juza M., Tintoré J. 2016. Subsurface circulation and mesoscale variability in the Algerian subbasin from altimeter-derived eddy trajectories. J. Geophys. Res. Oceans, 121: 6310-6322.
https://doi.org/10.1002/2016JC011760
Firing E., Hummon J.M. 2010. Shipboard ADCP Measurements. In: Hood, E.M., Sabine C.L., Sloyan B.M. (eds), The GO-SHIP Repeat Hydrography Manual: A Collection of Expert Reports and Guidelines. Version 1, 11pp. (IOCCP Report Number 14; ICPO Publication Series Number 134).
https://doi.org/10.25607/OBP-1352
Isern-Fontanet J., García-Ladona E., Font J. 2006. Vortices of the Mediterranean Sea: An Altimetric Perspective. J. Phy. Oceanogr. 36: 87-103.
https://doi.org/10.1175/JPO2826.1

Juza M., Escudier R., Vargas-Yáñez M., et al. 2019. Characterization of changes in Western Intermediate water properties enabled by an innovative geometry-based detection approach. J. Mar. Syst. 191: 1-12.
https://doi.org/10.1016/j.jmarsys.2018.11.003

Mallil K., Testor P., Bosse A., et al. 2022. The Levantine Intermediate Water in the Western Mediterranean and its interactions with the Algerian Gyres: insights from 60 years of observation. Ocean Sci. 18: 937-952,
https://doi.org/10.5194/os-18-937-2022

Millot C., Taupier-Letage I. 2005. Circulation in the Mediterranean Sea. In: Saliot, A. (eds) The Mediterranean Sea. Handbook of Environmental Chemistry, vol 5K. Springer, Berlin, Heidelberg,
https://doi.org/10.1007/b107143

Millot C., Benzohra M., Taupier-Letage I. 1997. Circulation off Algeria inferred from the Mediprod-5 current meters. Deep-Sea Research I, 44: 1467-1495.
https://doi.org/10.1016/S0967-0637(97)00016-2

Pinot J.-M., López-Jurado J. L. Riera M. 2002. The CANALES experiment (1996-1998). Interannual, seasonal, and mesoscale variability of the circulation in the Balearic Channels. Prog. Oceanogr. 55: 335-370.
https://doi.org/10.1016/S0079-6611(02)00139-8

Puillat I., Taupier-Letage I., Millot C. 2002. Algerian eddies lifetime can near 3 years, J. Mar. Syst. 31: 245-259.
https://doi.org/10.1016/S0924-7963(01)00056-2

Renault L., Orguz T., Pascual, A., Tintoré J. 2012. Surface circulation in the Alborán Sea (Western Mediterranean) inferred from remotely sensed data. J. Geophys. Res. Vol. 117, C08009.
https://doi.org/10.1029/2011JC007659

Ruiz S., Font J., Emelianov M., et al. 2002. Deep structure of an open-sea eddy in the Algerian Basin. J. Mar. Syst. 33-34: 179-195,
https://doi.org/10.1016/S0924-7963(02)00058-1

Sánchez-Garrido J.C., García-Lafuente J., Álvarez-Fanjul E., et al. 2013. What does cause the collapse of the Western Alboran Gyre? Results of an operational ocean model. Prog. Oceanogr. 116: 142-153,
https://doi.org/10.1016/j.pocean.2013.07.002

Schroeder K., Tanhua T., Chiggiato J., et al. 2023. The forcings of the Mediterranean Sea and the physical properties of its water masses, In: Schroeder K., Chiggiato J: (eds), Oceanography of the Mediterranean Sea: An introductory guide. Elsevier, Amsterdam,
https://doi.org/10.1016/B978-0-12-823692-5.00005-4

Scott R., Marsh R., Hays G. C. 2014. Ontogeny of long distance migration. Ecology, 95: 2840-2850.
https://doi.org/10.1890/13-2164.1

Testor P., Send U., Gascard J.-C., et al. 2005. The mean circulation of the southwestern Mediterranean Sea: Algerian gyres. J. Geophys. Res. 110: C11017,
https://doi.org/10.1029/2004JC002861

Troupin C., Pascual A., Ruiz S., et al. 2019. The AlborEx data set: sampling mesoscale features in the Alboran Sea. Earth Syst. Sci. Data. 11: 129-145.
https://doi.org/10.5194/essd-11-129-2019

Vargas-Yáñez M., García-Martínez M.C., Moya F., et al. 2017. Updating Temperature and Salinity Mean Values and Trends in the Western Mediterranean: The RADMED Project. Prog. Ocean. 157: 27-46.
https://doi.org/10.1016/j.pocean.2017.09.004

Vargas-Yáñez M., Juza M., Balbín R., et al. 2020. Climatological Hydrographic Properties and Water Mass Transports in the Balearic Channels from Repeated Observations Over 1996-2019. Front. Mar. Sci. 7:568602.
https://doi.org/10.3389/fmars.2020.568602

Vargas-Yáñez M., García-Martínez M.C., Moya F., et al. 2021a. The climatic and oceanographic context. In: Báez J.C., Vázquez J.T., Camiñas J.A. et al. (eds), Alborán Sea, Ecosystems and marine resources. Springer, Switzerland,
https://doi.org/10.1007/978-3-030-65516-7

Vargas-Yáñez M., Juza M., García-Martínez M.C., et al. 2021b. Long-Term Changes in the Water Mass Properties in the Balearic Channels Over the Period 1996-2019. Front. Mar. Sci. 8.
https://doi.org/10.3389/fmars.2021.640535

Viúdez A., Tintoré J. 1995. Time and space variability in the eastern Alboran Sea from March to May 1990. J. Geophys. Res. 100: 8571-8586,
https://doi.org/10.1029/94JC03129

Viúdez A., Tintoré J., Haney R. L. 1996. Circulation in the Alboran Sea as determined by Quasi-Synoptic hydrographic observations. Part I: Three-dimensional structure of the two anticyclonic gyres. J. Phys. Oceanogr. 26, 684-705,
https://doi.org/10.1175/1520-0485(1996)026<0684:CITASA>2.0.CO;2
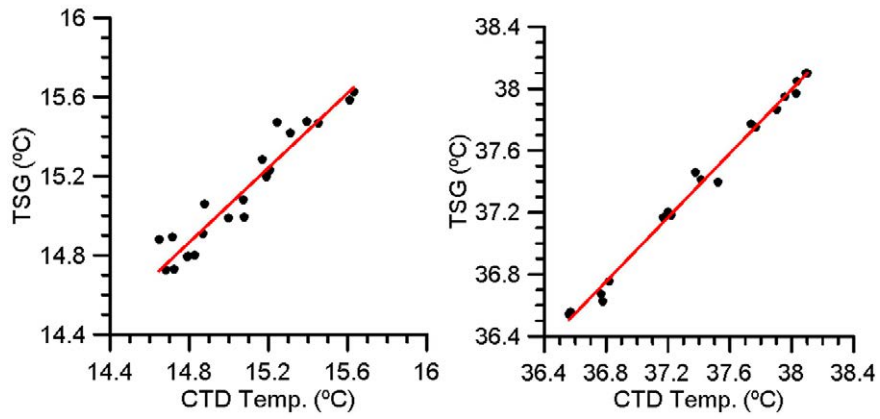
SUPPLEMENTARY MATERIAL

Fig. S1. – Regression of CTD surface temperature (left) and salinity (right) data on thermosalinograph data.
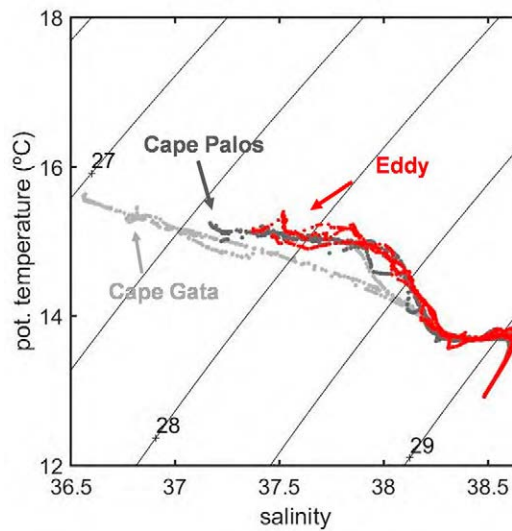

Fig. S2. – Red dots show the temperature-salinity diagram for the three oceanographic stations within the eddy (G1, G2 and G3). Grey dots show the temperature-salinity diagrams for those stations from the nearby transects to the south of Cape Palos and Cape Gata.